Numerical Investigation of Controllable Parameters Effect on Nanofluid Flooding in a Random Pore Generated Porous Medium

Gharibshahi, Reza; Jafari, Arezou*[+]

Chemical Engineering Department, Tarbiat Modares University, Tehran, I.R. IRAN

ABSTRACT: *This study simulates the enhanced oil recovery process using nanofluids into a microporous medium. To obtain the optimum values that affect this process, design experiments with the general factorial method was performed. Four parameters included type of nanoparticles and the base fluids, diameter and volume fraction of nanoparticle were considered. The porous medium was created with the commercial grid generation tool and Fluent software was used to solve the governing equations. Comparison of numerical results with the experimental data illustrates that they are in good agreement. In addition, results show that clay nanoparticles with formation water have the greatest impact on the oil recovery factor compared to other nanofluids. Also the nanofluid with higher amounts of nanoparticles in the base fluid and smaller diameter have better performance in improving the oil recovery factor. Therefore, for having the maximum oil recovery factor, the best combination of parameters is clay nanoparticles with 2 nm diameter and 5 vol. % in formation water.*

KEYWORDS: *Oil recovery factor; Nanofluid, CFD; Design experiment; General factorial; Optimization; Porous medium.*

INTRODUCTION

Nanoparticles as an effective bridge between bulk materials and atomic or molecular structures has been considered greatly in oil and gas industries [1-2]. Accordingly, one of the best practices of nanoparticles is their application for Enhanced Oil Recovery (EOR). Many mechanisms have been proposed for their contribution in the improvement of the oil recovery factor. Nanoparticles can change the wettability of rock reservoirs from oil-wet towards water-wet [3-8]. Furthermore, they can decrease the interfacial tension of trapped oil and water so that mobilize the oil ganglia [9-13]. In addition, nanoparticles can reduce the viscosity of heavy oils creating the more favorable mobility conditions for oil to be produced [14-16]. Moreover, they can facilitate an appropriate mobility ratio for the injected fluid which is resulted in improvement of sweep efficiency as well as reduction of the finger effect [17-20].

Different properties of an injected fluid such as density, viscosity, thermal conductivity and suchlike may be influenced by the addition of nanoparticles [17, 21]. In addition, there are many types of nanoparticles such as SiO_2, TiO_2, Al_2O_3, Fe_2O_3, and CuO as well as various

* *To whom correspondence should be addressed.*
+ *E-mail: ajafari@modares.ac.ir*
1021-9986/2021/3/780-795 16/$/6.06

basic fluids such as water, brine, formation water and ethanol [3, 22-24]. Considering such variety, selection of the best pair for the nanofluid injection is not simple. Therefore, adjustment of effective parameters in nanofluid flooding at optimum level is required to achieve higher oil recovery factors. In this work, it is facilitated through design of experiments (DOE) and simulation of the nanofluid flooding by Computational Fluid Dynamics (CFD).

DOE is comprised of different statistical and mathematical methodologies that aid researchers to plan minimum required tests among sample space for thoroughly understanding of the effects of screened important factors and their interactions on a specific process. Moreover, it can be used for optimization of the studied process [25].

CFD technique is a branch of fluid dynamics and is a common method to study and analyze problems that involve fluid flows. It can complete the efforts of experimental studies [26-27]. By running this method, simulation study of complex and difficult conditions is easily possible while preparation of these conditions for the experimental study may be a struggle [28-30]. This simulation technique has been used in many fields of the oil and gas sector such as drilling, erosion, design of equipment and EOR [31-33]. However, CFD simulation of the nanofluid injection for EOR objectives has not reported by other researchers.

Therefore, in this study, the nanofluid flooding in a 2D micromodel is simulated using a CFD approach and the numerical results is validated with the experimental data [5]. The micromodel apparatus has been selected in this research, because the fluid flow in it is visible [34-36]. Visualization of transport phenomena in porous media at pore scale, can help researchers to study the displacement behavior of phases in several processes. It is clear that different micromodels can be used for this purpose. But previous studies about the effect of pore morphology and its distribution in the micromodels indicate that the micromodel with random distribution of pores is suitable for investigation of the nanofluid flooding operations [37-39]. Furthermore, in such a micromodel the fluid flow pattern is the nearest one to the typical flow of two phase flow in real porous media and also fingering and trapping effects of the injected fluid can be observed approximately well. Therefore, in this study a micromodel with random distribution of pores selected as the porous medium.

Consequently, in this research a model is developed using general factorial design as one of the best methodologies of DOE for statistical analysis and optimization of the effective parameters on the oil recovery factor in the nanofluid flooding. The general factorial method is a multi-level, statistical and detailed method and usually used for extremely precise study. This method is recommended when the number of variables is limited. It should be mentioned that optimizing the effective parameters in nanofluid injection for improving the oil recovery has been done in this work for the first time.

NUMERICAL SECTION

Geometry creation

Gambit 2.3 (Fluent Inc.) software has been used to create the geometry of porous medium (Fig. 1). Dimensions of the pattern were $6\times6\times0.0065$ cm^3 according to the model had been designed for the experimental study [5]. Very low thickness of the micromodel confirms the assumption of a 2D geometry for the porous medium. Using a random generation code in Matlab and C++, distribution of 123 random non-overlapping circles with radius 0.25 cm was carried out in the pattern. In other words, circles did not place out of the square border. After subtracting the circles surface area from the main domain, the porosity of designed pattern was calculated as 0.33.

The boundary conditions were velocity inlet and pressure outlet for the inlet and outlet ports, respectively. Other edges due to no input and output flow in/from them were considered as wall.

Grid independency check

(Tri/pave) mesh type was used for meshing the created geometry. Inlet and outlet ports were meshed with a smaller size than other edges. It was done to increase the accuracy of calculations nearby. To obtain a better visualization of the generated mesh, Fig. 1 shows the magnified inlet and outlet zones of the porous medium. To investigate that results are grid independent, three types of grids produced containing different mesh sizes. Then the governing equations for each grid were solved with Fluent software at flow rate 8×10^{-4} cc/min and $\Delta t=0.1$ s. Iterations continued until all residuals in any grid reached to the steady state. Total pressure at the inlet and outlet were calculated and the pressure drop as the numerical result

Table 1: Results of the grid independency test.

No.	Mesh Size			No. of Cells	No. of Nodes	ΔP (Pa.)	Relative Error (%)
	Inlet and Outlet	Other Edge	Face				
Grid 1	0.01	0.015	0.02	125469	78546	0.87	6.17
Grid 2	0.008	0.01	0.02	251433	136449	0.93	
Grid 3	0.005	0.008	0.02	445385	212545	0.96	2.89

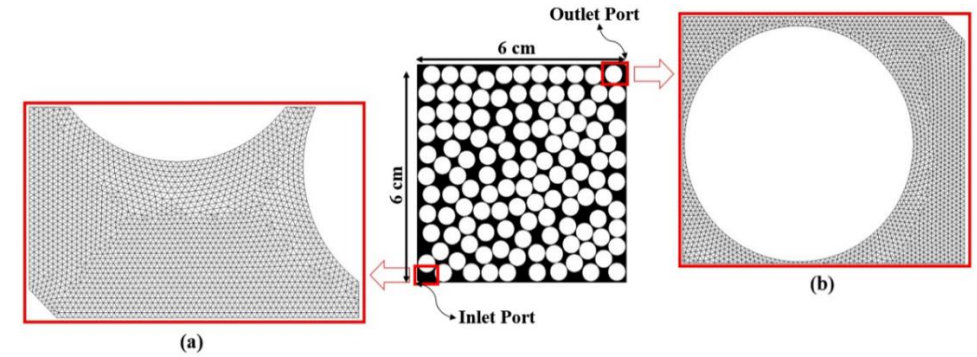

Fig. 1: Schematic geometry of the porous medium and magnified zones of the meshed geometry for better visualization; (a) inlet port, (b) outlet port.

has been chosen to determine the amount of error between each two grids. Results of investigations which are tabulated in Table 1 reveal that the relative error between grid 2 and 3 is less than 3%. Therefore, to save time and computational cost the grid comprising 251433 cells (grid 2) was chosen as the main grid.

Governing Equations

Injection of a fluid with specific properties for the enhanced oil recovery is a multiphase flow type. The first step in solving the multiphase flow is characterization of the flow regime. Fluent has several multiphase models for this purpose. Mixture model is a simplified model that can be used to model multiphase flows where the phases have different speeds. As well as, it can be used for modeling homogenous multiphase flows where phases influence on each other very much while the velocity of the phases are the same. It can model n phases (fluids or particulates) by solving the continuity and momentum equations for the mixture. Another advantage of the mixture model is that it has a module named granular that is able to define the diameter of nanoparticles. It is obvious that nanoparticles diameter is an important parameter that has influence on nanoparticles trapping at throats and consequently closing the oil pathways to the production well (exit port).

The mixture model solves the continuity, momentum and energy equations for the mixture as well as a volume fraction equation for the secondary phases [40, 41]. Conservation of mass, momentum and volume fraction, microscopic governing equations, are as follows:

$$\frac{\partial}{\partial t}(\rho_m) + \nabla.(\rho_m \vec{V}_m) = 0 \quad (1)$$

$$\frac{\partial}{\partial t}(\rho_m \vec{V}_m) + \nabla.(\rho_m \vec{V}_m \vec{V}_m) = -\nabla P_m + \nabla.(\mu_m \nabla \vec{V}_m) + \vec{F} + \nabla.(\sum_{k=1}^{n} \varphi_k \rho_k \vec{V}_{dr,k} \vec{V}_{dr,k}) \quad (2)$$

$$\frac{\partial}{\partial t}(\varphi_p \rho_p) + \nabla.(\varphi_p \rho_p \vec{V}_m) = -\nabla.(\varphi_p \rho_p \vec{V}_{dr,p}) \quad (3)$$

Where the mixture velocity, density and viscosity respectively are:

$$\vec{V}_m = \frac{\sum_{k=1}^{n} \varphi_k \rho_k \vec{V}_k}{\rho_m} \quad (4)$$

$$\rho_m = \sum_{k=1}^{n} \varphi_k \rho_k \quad (5)$$

$$\mu_m = \sum_{k=1}^{n} \varphi_k \mu_k \quad (6)$$

The drift velocity of k^{th} phase is:

$$\vec{V}_{dr,k} = \vec{V}_k - \vec{V}_m \quad (7)$$

The slip velocity (relative velocity) is defined as the velocity of a secondary phase (p) relative to the primary phase (f) velocity:

$$\vec{V}_{pf} = \vec{V}_p - \vec{V}_f \quad (8)$$

In these study oil and nanofluid were assumes as the primary and secondary phases, respectively. The drift velocity is related to the relative velocity is:

$$\vec{V}_{dr,p} = \vec{V}_{pf} - \sum_{k=1}^{n} \frac{\varphi_k \rho_k}{\rho_{eff.}} \vec{V}_{fk} \quad (9)$$

For more information about this model, see [27]. The under-relaxation factors for pressure were assigned as 0.9, for density=1, for body forces=1, for momentum=0.1, for slip velocity=0.1 and for volume fraction was 0.2. Equations of mass and momentum must be satisfied to achieve a reasonable rate of convergence that it occurs when the normalized residuals become smaller than 0.001.

Investigation of the effective parameters

A general factorial design has been developed to investigate the effects of important parameters and their interactions on the efficiency of nanofluid flooding as the corresponding response. Then it was used to find the optimum arrangement of parameters by means of which the oil recovery factor become maximum. The first step is selection of effective parameters. Considering different criteria presented in the literature related to nanoparticles contribution in EOR applications, seven primarily parameters were determined included: type of nanoparticle, type of the base fluid, diameter of nanoparticles, volume fraction of nanoparticles in the base fluid, the nanofluid injection rate, type of oil, and finally initial oil saturation. The number of effective parameters exceeded a conventional DOE plan. Therefore, screening of selected parameters was carried out according to the available experimental data. Finally four parameters were screened whose ranges are tabulated in Table 2.

Diameter of nanoparticles was varied in the range 5-50 nm (because greater than this size, problems such as nanoparticle trapping at pore throat and sedimentation in the porous medium occurs) and volume fraction of nanoparticles in the base fluid was in the range 0.5-5 vol. %. Three types of nanoparticles included silica, titanium and clay were considered accompanied by three types of fluid included water, ethanol and formation water as the base fluid. Other parameters were determined as follows:

1- By considering different criteria such as recovery, time and turbulency effect, the injection flow rate 0.0006 cc/min (1.2 ft/day) was chosen as the optimum value [36, 42]. This optimum value is near to the fluid velocity in underground oil reservoirs.

2- A heavy crude oil with API 19° was used as the hydrocarbon phase.

3- Because applying the initial oil saturation in simulations can be done in different methods, this factor has been neglected. In other words, investigation of this parameter needs a separate research, so here no initial water saturation was considered.

To design the required simulation runs, Design Expert 7 was used.

Temperature of the porous medium as well as all of the streams considered as 25°c in accordance with the experimental work [5]. Physical properties of the crude oil and base fluids were calculated in this temperature [43] which are shown in Table 3.

Density and molecular weight of nanoparticles determined based on the available data in Handbooks [44] while other properties calculated by the kinetic theory equation. Physical properties of nanoparticles are presented in Table 4.

RESULTS AND DISCUSSION

Validation of Numerical Results

To validate the accuracy of numerical results, oil recovery factor of the nanofluid (4 vol. % silica nanoparticles) injection predicted by CFD was compared to available experimental data [5] as shown in Fig. 2.

Firstly, the porous medium was saturated with the oil and two phase flow and steady state condition were assumed. In addition, mixture model was used to solve the governing equations. All simulations were performed at ambient

Table 2: Effective parameters and their levels used in the nanofluid flooding.

Parameter	Type	Level 1	Level 2	Level 3
A: Type of nanoparticle	Categorical	silica	titanium	clay
B: Type of base fluid	Categorical	water	Ethanol	Formation water
C: Diameter of nanoparticle (nm)	Numerical	2	50	-
D: Concentration of nanoparticle (Vol. %)	Numerical	0.5	5	-

Table 3: Physical properties of fluids at 25 °C.

Phase	Property	Value
Formation water	Density, ρ (kg/m^3)	1110
	Viscosity, μ (kg/m.s)	0.0017
	Heat capacity, Cp (J/kg.K)	4000
	Thermal conductivity, k (w/m.K)	0.6
Water	Density, ρ (kg/m^3)	998.2
	Viscosity, μ (kg/m.s)	0.00089
	Heat capacity, Cp (J/kg.K)	4182
	Thermal conductivity, k (w/m.K)	0.61
Ethanol	Density, ρ (kg/m^3)	785
	Viscosity, μ (kg/m.s)	0.001074
	Heat capacity, Cp (J/kg.K)	2470
	Thermal conductivity, k (w/m.K)	0.182
Crude oil	Density, ρ (kg/m^3)	933
	Viscosity, μ (kg/m.s)	0.87
	Molecular weight, Mw (kg/kmol)	583.725

Table 4: Physical properties of nanoparticles at 25 °C.

Nanoparticle	Property	Value
Clay	Density, ρ (kg/m^3)	6000
	Molecular weight, Mw (kg/kmol)	180.1
Silica	Density, ρ (kg/m^3)	2400
	Molecular weight, Mw (kg/kmol)	60.08
Titanium	Density, ρ (kg/m^3)	4230
	Molecular weight, Mw (kg/kmol)	79.866

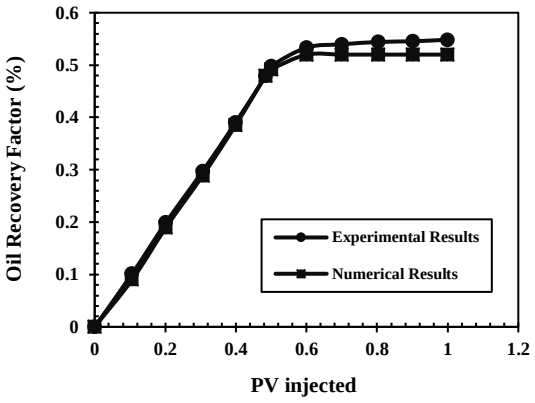

Fig. 2: Comparison of numerical results with the experimental data.

pressure and temperature with flow rate 0.0006 cc/min. The effect of different time intervals (0.01, 0.1 and 1 s) on numerical results accuracy were tested and finally to save time and computational cost, Δt=0.1s has been selected for all simulations. Because the oil recovery factor for Δt=0.1s and Δt=0.01s was approximately the same. In other words, the relative error between these two time intervals was not considerable. The oil recovery factor in the nanofluid injection and after 10000s was determined as the ultimate oil recovery factor. Fig. 2 shows that simulation results are in a good agreement with experimental data. The relative error between the ultimate oil recovery factors was calculated as 5.17%. Fig. 3 shows the nanofluid volume fraction contours in the porous medium with passing time. From the figure it is clear that the fluid flow pattern in the generated geometry is the same as the fluid flow in actual rock reservoirs. So the fingering effect can be studied in this porous medium as well. Breakthrough occurs at 3666 s after the nanofluid injection and the oil recovery factor at the breakthrough time is 31.86%. In addition, the difference between the ultimate oil recovery factor and the recovery at breakthrough time is 20.14%.

Parametric Study and Optimization Results

General factorial design (Design Expert software) was used to plan a systematic study. This method in comparison with conventional ones needs fewer tests to optimize a process. Designed experiments as terms of selected factors and their corresponding responses are tabulated in Table 5.

Each run was carried out by Fluent and the relevant oil recovery factor after 10000s was determined as the corresponding response. A 2FI statistical model was developed to predict the responses. It is worthy to mention that in 2FI model, the interactions between two factors such as AB, BC and etc. can be considered in the predicted model. The analysis of variance (ANOVA) for this model is shown in Table 6.

There are different parameters for statistical analysis of the developed model. First of all, degree of freedom for each parameter defined as:

$$DOF = n - 1 \tag{10}$$

Where *n* is the number of levels for each factor in the system. The second column of Table 6 is the sum of squares for each factor which is defined as:

$$S = \sum_{j=1}^{n} n.\left(m_j - m_t\right)^2 \tag{11}$$

Where m_j the standard is average of the results at level j for each factor and m_t is the total standard average. Another important factor is mean square for each factor (V) which is calculated as the sum of squares divided by its degrees of freedom as follows:

$$V = \frac{S}{DOF} \tag{12}$$

The variance ratio (F value) is the ratio of variance caused by the effect of a factor and variance from the error term. Accordingly, p-value is the probability of obtaining a test statistic result at least as extreme or as close to the one that was actually observed, assuming that the null hypothesis is true [45]. These two parameters determine the importance of factors where more significant factors have higher F values and lower p values [46].

ANOVA table indicates that 2FI model is significant with 95% confidence because the p-value of the model has been calculated less than 0.05. This model was reduced to keep just significant terms. It seems that factor D (volume fraction of nanoparticle in the base fluid) has the greatest effect on the response of the system. Detailed statistical analysis of ANOVA table is summarized in Table 7.

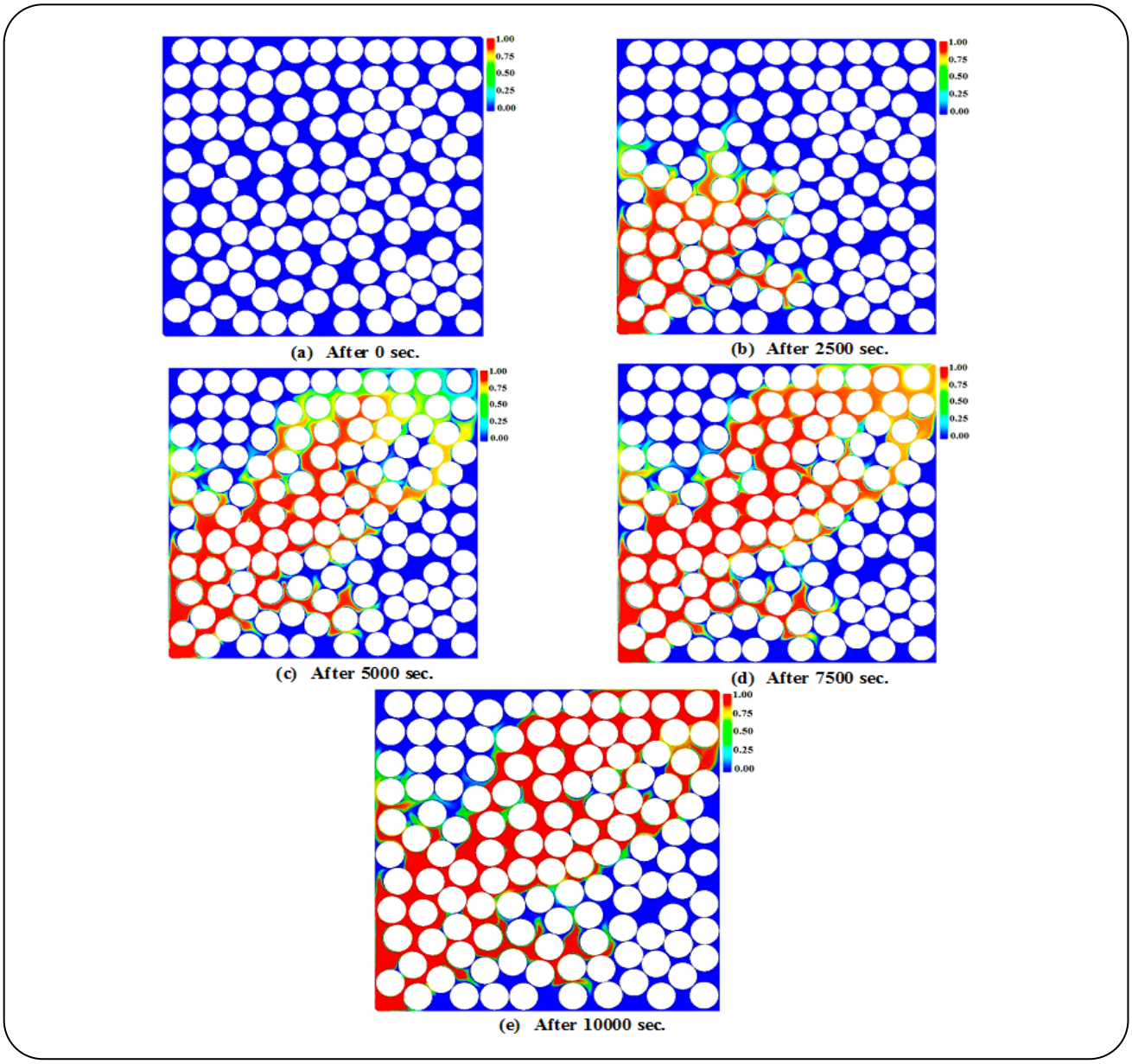

Fig. 3: The nanofluid volume fraction contours at different times of the injection.

The fitted correlation is significant (p-value<0.0001). The high values for the predicted and adjusted R^2 indicate that the reduced 2FI model has a good representation of the system. Adequate precision measures the signal to noise ratio and values more than 4 are favorable. Coefficient of variance (CV%) measures the reproducibility of the model. It defines as standard deviation divided by the mean value which is expressed as percentage. The CV for the developed model was calculated as 0.48%. In general, the values less than 10% imply that the fitted models are reasonably reproducible.

Values predicted by the statistical model versus actual values obtained by CFD simulation has been shown in the Fig. 4. According to this figure, it can be found that the model has been fitted very well by the simulation data. Because approximately whole points are located around the diagonal line.

For each type of nanoparticles and base fluids, models presented by the software based on the actual values for each parameter has been shown in Table 8. Using these models, the oil recovery factor at any nanoparticles diameter and volume fraction can be determined for each nanofluid.

Table 5: General factorial design developed for systematic study of the nanofluid injection.

No.	Type of Nanoparticle	Type of Base Fluid	Diameter (nm)	Volume Fraction (vol. %)	Ultimate Oil Recovery Factor
1	SiO_2	Water	50	5	54.36
2	Clay	Water	50	0.5	48.65
3	SiO_2	Water	50	0.5	48.14
4	TiO_2	Water	2	0.5	49.05
5	Clay	Ethanol	50	0.5	49.34
6	Clay	Formation Water	50	0.5	49.91
7	Clay	Water	2	5	55.87
8	TiO_2	Water	2	5	56.48
9	Clay	Water	2	0.5	49.95
10	SiO_2	Ethanol	50	5	55.24
11	Clay	Formation Water	50	5	56.96
12	Clay	Ethanol	50	5	56.3
13	SiO_2	Ethanol	50	0.5	48.86
14	SiO_2	Formation Water	50	0.5	49.32
15	SiO_2	Water	2	0.5	48.67
16	TiO_2	Ethanol	2	5	56.03
17	SiO_2	Ethanol	2	5	55.98
18	TiO_2	Ethanol	50	5	55.41
19	Clay	Ethanol	2	5	56.62
20	TiO_2	Formation Water	2	0.5	48.78
21	Clay	Formation Water	2	5	57.34
22	Clay	Ethanol	2	0.5	49.76
23	Clay	Formation Water	2	0.5	50.02
24	SiO_2	Formation Water	2	5	56.43
25	SiO_2	Ethanol	2	0.5	49.12
26	TiO_2	Ethanol	50	0.5	48.95
27	Clay	Water	50	5	55.42
28	TiO_2	Ethanol	2	0.5	49.23
29	TiO_2	Formation Water	50	0.5	49.44
30	SiO_2	Water	2	5	55.12
31	TiO_2	Formation Water	50	5	55.99
32	SiO_2	Formation Water	50	5	55.87
33	TiO_2	Water	50	5	54.58
34	TiO_2	Formation Water	2	5	56.58
35	SiO_2	Formation Water	2	0.5	49.88
36	TiO_2	Water	50	0.5	48.24

Table 6: ANOVA analysis for the reduced 2FI model.

Source	Sum of Squares	DOF	Mean Square	F Value	p-value
Model	421.97	8	52.75	813.00	< 0.0001
A-type of nanoparticle	3.93	2	1.96	30.25	0.0038
B-type of base fluid	6.00	2	3.00	46.21	0.0017
C-dp	2.74	1	2.74	42.22	0.0029
D-volume fraction	408.51	1	408.51	6296.63	< 0.0001
BC	0.79	2	0.40	6.12	0.0606
Residual	0.26	4	0.06		
Cor Total	422.23	12			

Table 7: Statistical results of the ANOVA for the reduced 2FI model.

Response	Final Equation in Terms of Coded Factors	p-value	R^2	Adj. R^2	Adequate precision	CV %
Oil recovery factor	+52.55-0.30A[1]-0.16A[2]-0.51B[1]+ 0.018B[2]-0.28C+3.37D-0.20B[1]C+ 0.056B[2]C	< 0.0001	0.9994	0.9982	71.504	0.48

Table 8: Presented models by the software.

Type of nanoparticle	Type of base fluid	Model
Silica	Water	48.14-0.02×C+1.50×D
Silica	Ethanol	$48.38-9.17\times10^{-3}\times C+1.50\times D$
Silica	Formation Water	$48.76-5.35\times10^{-3}\times C+1.50\times D$
Titanium Oxide	Water	48.29-0.02×C+1.50×D
Titanium Oxide	Ethanol	$48.53-9.17\times10^{-3}\times C+1.50\times D$
Titanium Oxide	Formation Water	$48.90-5.35\times10^{-3}\times C+1.50\times D$
Clay	Water	48.90-0.02×C+1.50×D
Clay	Ethanol	$49.15-9.17\times10^{-3}\times C+1.50\times D$
Clay	Formation Water	$49.52-5.35\times10^{-3}\times C+1.50\times D$

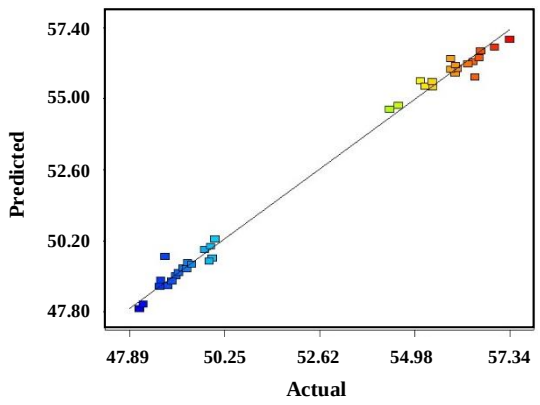

Fig. 4: Predicted values versus actual data of the oil recovery factor.

Effect of Nanoparticle Type

Fig. 5 (a) shows the effect of each individual nanoparticle on the oil recovery factor. It can be seen that clay nanoparticles has the highest efficiency for the oil recovery [47]. High density of clay nanoparticles causes less amount of material required for the nanofluid injection. Therefore, density and viscosity of the base fluid adjusted at an appropriate level as well as lower aggregation and impaction are occurred in the porous medium. It means that the fluid front flows more favorable in the created geometry and less permeability reduction occurs in the porous bed after the nanofluid flooding. On the other hand, it should be borne in mind that the clay

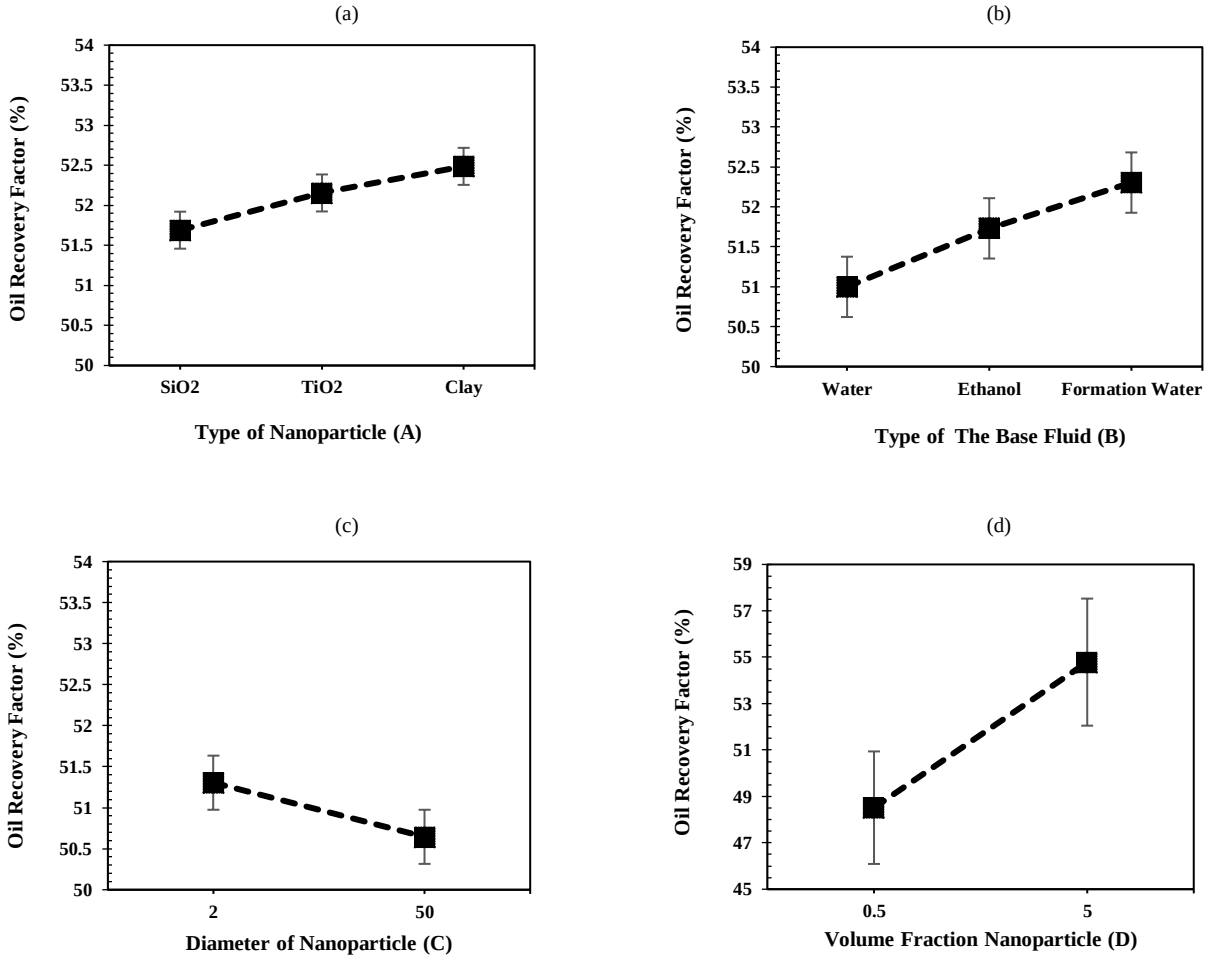

Fig. 5: Effect of Parameters on the oil recovery factor, (a) type of nanoparticles, (b) type of the base fluid, (c) diameter of nanoparticles and (d) volume fraction of nanoparticles.

nanoparticles have an inorganic origin and because these particles are connatural with many reservoirs such as sandstone and so on, they can be highly compatible with reservoirs during the injection process. Therefore, it seems that clay nanoparticles have high potential for use in EOR processes. It was also observed that the effect of titanium oxide nanoparticles is higher than silica nanoparticles. This is due to the optimal rheological properties of titanium oxide nanofluid and results in a better mobility ratio in comparison with silica nanofluid as injected fluid.

Effect of the Base Fluid Type

Numerical results on the oil recovery factor and related to the base fluid type have been presented in Fig. 5 (b). As the figure illustrates the formation water is the best choice compared to ethanol and water. Moreover, the effect of ethanol on the oil recovery factor is more than water. This is due to the greater ability of formation water and ethanol fluids to reduce interfacial tension between injecting fluid and oil than water. Also, it can be attributed to the better adjusting mobility ratio of injected fluid by adding nanoparticles to the formation water, ethanol and water, respectively [47]. It should be mentioned that these results are in a good agreement with experimental work of *ogolo et al.* [3]. They concluded that nanofluids prepared by distilled water have low oil recovery factor while brine gives a good result. Also they found that dispersion of silica nanoparticles in ethanol compared to distilled water caused an enhancement in the oil recovery factor.

Effect of Nanoparticles Diameter

Fig. 5 (c) depicted how the diameter of nanoparticles influences on the efficiency of nanofluid injection. It was

found that the oil recovery factor increases with diameter reduction of nanoparticles. In this conditions, transfer of nanoparticles as well as prevention of entrapment in the porous medium were performed better. As a result, the permeability reduction during nanofluids flooding in the porous medium will decrease and the injected fluid can cover more surfaces of the bed, so the oil recovery improves. By increasing the diameter of nanoparticles problems such as entrapment at pores throat arise. Therefore, the probability of oil reservoir permeability reduction after nanofluid injection in order to improve oil recovery is increased. This causes damage to the oil formation and reduces oil production from the reservoir in the long run. Smooth slope of the diagram presented in Fig. 5 (c) indicates that the overall effects of variation in this range are less than other factors. It is worthy to mention that the influence of nanoparticles diameter in the nanofluid flooding has not been reported before.

Effect of Nanoparticles Volume Fraction in the Base Fluid

According to Fig. 5 (d), higher oil recovery factors are achieved when the volume fraction of nanoparticles in the base fluid increases. Sharp slope of this figure indicates the high effect of this factor on the oil recovery factor compared to previous parameters. Because by addition of nanoparticles to a base fluid, properties of the base fluid change and adjust at a suitable level. In other words, with density and viscosity alteration of the base fluid, the mobility ratio of the injected fluid improves and in the flooding operations the nanofluid will flow more uniform and higher surface of the porous medium will be in contact with the injected fluid [48]. So the oil recovery factor increases and much more oil can be produced from the reservoir.

Parameters Interaction

Considering to the parameters interactions between two factors is valuable. Also studying about a relationship among three parameters that may occur is more worthy. Investigation of results illustrated that in the present model, there exists an interaction between two parameters (type of the base fluid (B) and nanoparticles diameter (C)). Fig. 6 shows the interaction effect between these parameters for silica nanoparticles and at different levels of parameter D. According to this figure it can be obtained

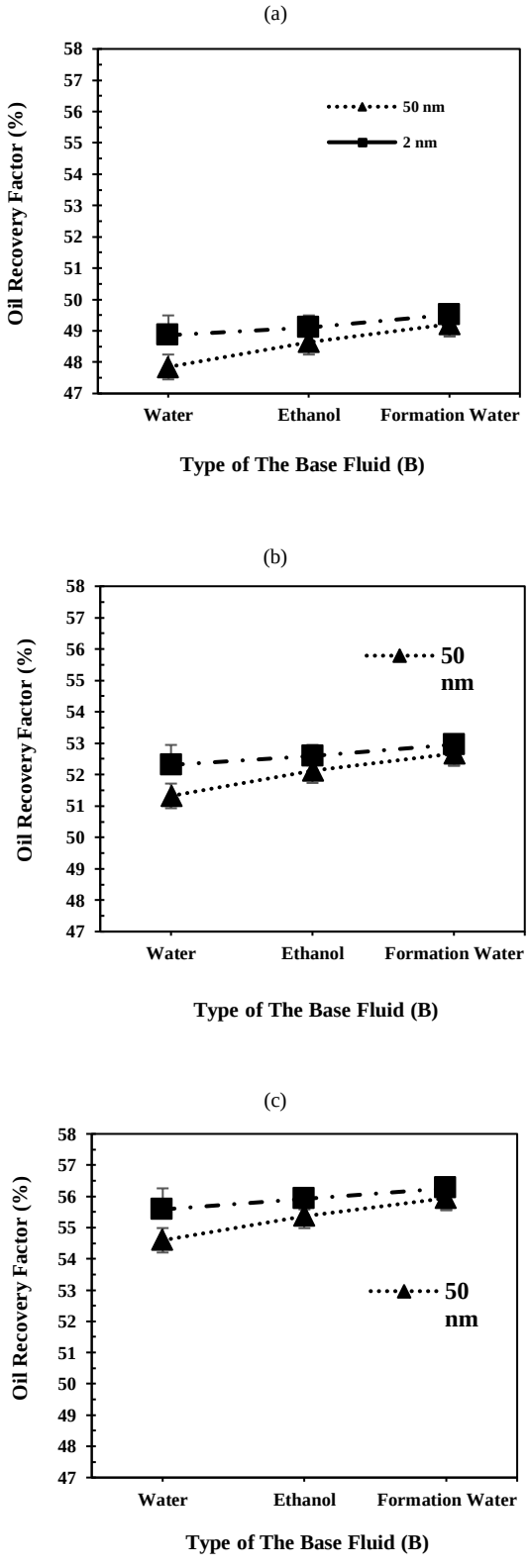

Fig. 6: Interaction of parameters B and C at (a) 0.5 vol. %, (b) 2.75 vol. % and (c) 5 vol. % nanoparticles in the base fluid.

that nanoparticles diameter has a lower influence on the system response, but nanoparticles volume fraction in the base fluid has the greatest impact on the oil recovery factor compared to other parameters.

By considering the interactions between two parameters B and C, Fig. 7 shows the interaction effect between these parameters for SiO_2, TiO_2 and clay nanoparticles at constant volume fraction of nanoparticles (2.75 vol. %). From this figure it can be found that at constant nanoparticles' volume fraction in the base fluid, SiO_2 and TiO_2 nanoparticles approximately have the same oil recovery factor. However, TiO_2 nanoparticles have more ability to recover oil, and clay nanoparticle has the most oil recovery factor. Also it can be seen that decreasing the diameter of nanoparticles enhances the oil recovery factor and as well as this parameter has a lower impaction on this process.

Determination of Optimum Conditions and Confirmatory Test

One of the best advantages with design of experiments methodologies is ability to optimize the processes and in this study, the purpose of nanofluid injection into the porous medium is to maximize the oil recovery factor. For this aim, goal of factors was selected as "in range" while "maximum" was considered as the proper response. To obtain the maximum process response, the best combination of factors as optimum conditions was recommended by the model and is tabulated in Table 9.

To check the validity of optimized conditions given by the model, a confirmation test was carried out by applying the optimum level for each factor. Result of the CFD simulation conducted at the optimal conditions was shown in Table 10. It is clear that the oil recovery factor of the verification test and its corresponding predicted value obtained from fitted correlations are in close agreement at a 95% confidence interval. Results obtained by optimal run, show that the oil recovery factor is 57.34 which is in the predicted range. These results confirmed validity of the model and the numerical values were determined to be near the predicted values.

CONCLUSIONS

A computational fluid dynamics method was developed to simulate nanofluids transport in a 2D micro porous medium. The fluid flow in a porous medium was

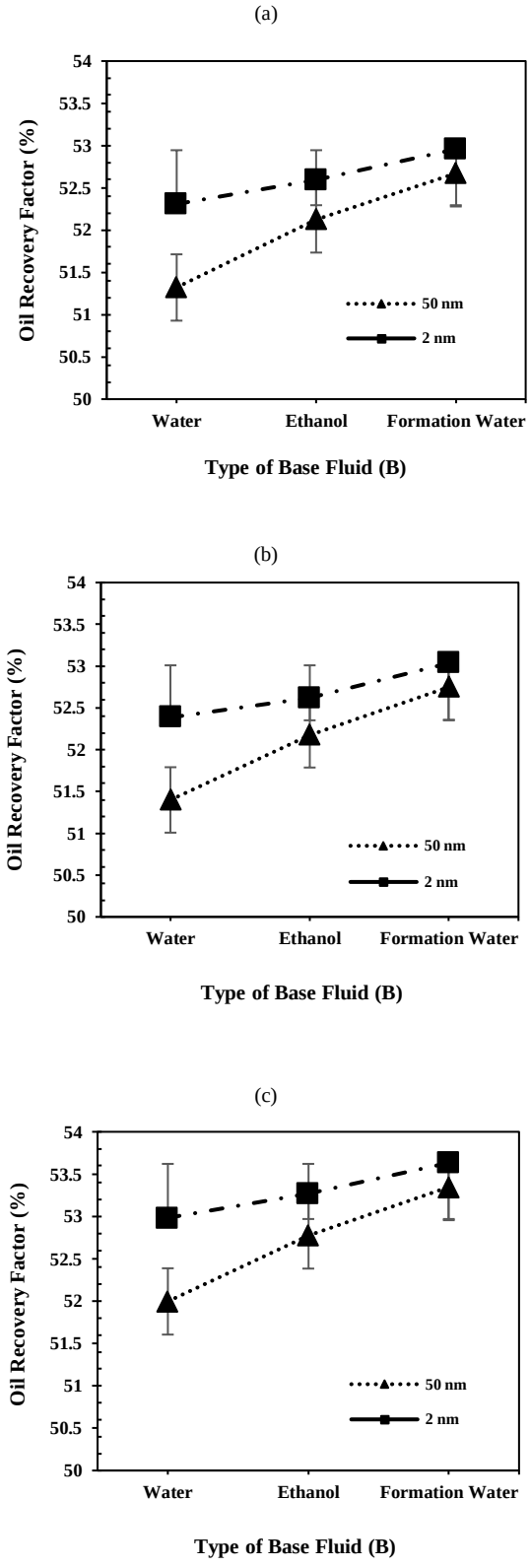

Fig. 7: Interaction of parameters B and C for (a) SiO2, (b) TiO2 and (c) clay nanoparticles at 2.75 vol. %.

Table 9: Optimal conditions to obtain the highest oil recovery factor in the nanofluid injection.

Type of Nanoparticle	Type o the Base Fluid	Diameter (nm)	Volume Fraction (vol. %)	Oil Recovery Factor (%)
Clay	Formation water	2	5	56.99

Table 10: Point prediction in order to verify the response at optimal conditions.

Response	Prediction	Confirmation Test	95% CI low	95% CI high
Oil recovery factor (%)	56.99	57.34	56.60	57.93

investigated numerically using the multi-phase model. Gambit 2.3 was used to create the geometry and Fluent software was applied to solve momentum, continuity and volume fraction equations. The validity of numerical results was established by comparing them with the experimental data. Design expert software was used to investigate parameters effects in the nanofluid flooding and find the best combination of factors to obtain the maximum oil recovery factor. In overall the following results were obtained:

- Clay nanoparticles have the most effect on the oil recovery factor. Titanium oxide and silica nanoparticles, respectively are in the second and third order.

- Formation water compared to ethanol and water has the greatest impact on the oil recovery. Also the effect of ethanol is more than water.

- Whatever diameter of nanoparticles be smaller, they can move more easily in the porous medium without entrapping, so the oil recovery factor increases.

- By increasing nanoparticles volume fraction in the base fluid, the oil recovery factor improves. In addition, it is worthy to mention that this parameter compared to other factors has a greatest impact on the oil recovery factor.

- The optimal level for each parameter to obtain the maximum oil recovery factor is combination of clay nanoparticles, formation water, smaller diameter (2 nm) and greater volume fraction (5 vol. %) of nanoparticles.

Acknowledgment

The authors would like to thank Tarbiat Modares University and department of chemical engineering for laboratory facilities and Iran Nanotechnology Initiative Council and Iran National Elites Foundation for the financial support and Stat-Ease, Minneapolis, USA, for the provision of the Design-Expert package. Also authors have the best regards to Dr. S.M. Mousavi for the technical support in design experiment section.

Nomenclature

CV	Coefficient of variance
DOF	Degree of freedom
m_j	The standard average of the results at level j
m_t	The total standard average
n	Number of levels
S	Sum of squares
S_{wi}	Initial water saturation
V	mean square
$\vec{V}_{dr,k}$	Drift velocity of k^{th} phase
$\vec{V}_{dr,p}$	Drift velocity of a secondary phase
$\vec{V}_f$	Velocity of the primary phase
$\vec{V}_k$	Velocity of k^{th} phase
$\vec{V}_m$	Mixture velocity
$\vec{V}_p$	Velocity of a secondary phase
$\vec{V}_{pf}$	Slip velocity

Greek Letters

ΔP	Pressure difference between the inlet and outlet with finer mesh
Δt	Time step
μ_k	Viscosity of a k^{th} phase
μ_m	Mixture viscosity
μ_p	Viscosity of a secondary phase
ρ_k	Density of a k^{th} phase
ρ_m	Mixture density
ρ_p	Density of a secondary phase
φ	Volume fraction of a k^{th} phase
φ	Volume fraction of a secondary phase

Subscripts

dr	Drift
f	Primary phase
k	k^{th} phase

m	Mixture
p	Secondary phase

Received : Jun. 24, 2020 ; Accepted : Oct. 26, 2019

REFERENCES

[1] Ayatollahi S., Zerafat M., Nanotechnology-Assisted EOR Techniques: New Solutions to Old Challenges, *"SPE International Oilfield Nanotechnology Conference"*, Noordwijk, The Netherlands, 1-15 (2012).

[2] Kong X., Ohadi M.M., Petroleum T., Xiangling K., Applications of Micro and Nano Technologies in the Oil and Gas Industry-Overview of the Recent Progress, *"Abu Dhabi International Petroleum Exhibition and Conference"*, Abu Dhabi, UAE (2010).

[3] Ogolo N.A., Olafuyi O.A., Onyekonwu M.O., Enhanced Oil Recovery Using Nanoparticles, *"SPE Saudi Arabia Section Technical Symposium and Exhibition"*, Al-Khobar, Saudi Arabia (2012).

[4] Ju B., Fan T., Ma M., Enhanced Oil Recovery by Flooding with Hydrophilic Nanoparticles, *China Particuology*, **4(1)**: 41–46 (2006).

[5] Maghzi A., Mohammadi S., Ghazanfari M.H., Kharrat R., Masihi M., Monitoring Wettability Alteration by Silica Nanoparticles During Water Flooding to Heavy Oils in Five-Spot Systems: a Pore-Level Investigation, *Exp. Therm. Fluid Sci.*, **40**: 168–176 (2012).

[6] Roustaei A., Moghadasi J., Bagherzadeh H., Shahrabadi A., An Experimental Investigation of Polysilicon Nanoparticles' Recovery Efficiencies through Changes in Interfacial Tension and Wettability Alteration, *"SPE International Oilfield Nanotechnology Conference"*, Noordwijk, The Netherlands (2012).

[7] Nazari Moghaddam R., Bahramian A., Fakhroueian Z., Karimi A., Arya S., Comparative Study of Using Nanoparticles for Enhanced Oil Recovery: Wettability Alteration of Carbonate Rocks, *Energy & Fuels*, **29(4)**: 2111–2119 (2015).

[8] Hendraningrat L., Torsæter O., Effects of the Initial Rock Wettability on Silica-Based Nanofluid-Enhanced Oil Recovery Processes at Reservoir Temperatures, *Energy & Fuels*, **28(10)**: 6228–6241 (2014).

[9] Hendraningrat L., Shidong L., Torsæter O., A Glass Micromodel Experimental Study of Hydrophilic Nanoparticles Retention for EOR Project, *"SPE Russian Oil and Gas Exploration and Production Technical Conference and Exhibition"*, Moscow, Russia (2012).

[10] Skauge T., Hetland S., Spildo K., Skauge A., Cipr U., Nano-Sized particles for EOR, *"SPE Improved Oil Recovery Symposium"*, Tulsa, Oklahoma, USA, 24–28 (2010).

[11] Hendraningrat L., Engeset B.B., Suwarno S., Torsæter O., Improved Oil Recovery by Nanofluids Flooding: An Experimental Study, *"SPE Kuwait International Petroleum Conference and Exhibition"*, Kuwait City, Kuwait (2012).

[12] Parvazdavani M., Kiani S., Abbasi S., Synthesis and Experimental-Modelling Evaluation of Nanoparticles Movements by Novel Surfactant on Water Injection: An Approach on Mechanical Formation Damage Control and Pore Size Distribution, *Iran. J. Chem. Chem. Eng (IJCCE).*, **39(1)**: 209–223 (2018).

[13] Sun Q., Li Z., Li S., Jiang L., Wang J., Wang P., Utilization of Surfactant-Stabilized foam for Enhanced Oil Recovery by Adding Nanoparticles, *Energy & Fuels*, **28(4)**: 2384–2394 (2014).

[14] Qiu F., The Potential Applications in Heavy Oil EOR with the Nanoparticle and Surfactant Stabilized Solvent-Based Emulsion, *"Canadian Unconventional Resources and International Petroleum Conference"*, Calgary, Alberta, Canada, 1–12 (2010).

[15] Shah R., Application of Nanoparticle Saturated Injectant Gases for EOR of Heavy Oils, *"SPE Annual Technical Conference and Exhibition"*, New Orleans, Louisiana, USA (2009).

[16] Ehtesabi H., Ahadian M.M., Taghikhani V., Ghazanfari M.H., Enhanced Heavy Oil Recovery in Sandstone Cores using TiO_2 Nanofluids, *Energy & Fuels*, **28(1)**: 423–430 (2013).

[17] Fletcher A.J.P., Davis J.P., How EOR can be Transformed by Nanotechnology, *"SPE Improved Oil Recovery Symposium"*, Tulsa, Oklahoma, USA, 24–28 (2010).

[18] Haroun M. M., Ansari A., Al Kindy N., Sayed N.A., Ali B., Sarma H., Alhassan S., Al Kindy N., Abou Sayed N., Abdul Kareem B., Smart Nano-EOR Process for Abu Dhabi Carbonate Reservoirs, *"Abu Dhabi International Petroleum Conference and Exhibition"*, Abu Dhabi, UAE (2012).

[19] Yu J., An C., Mo D., Liu N., Lee R., Foam Mobility Control for Nanoparticle-Stabilized Supercritical CO2 Foam, *"SPE Improved Oil Recovery Symposium"*, Tulsa, Oklahoma, USA, 1–13 (2012).

[20] Ehtesabi H., Ahadian M.M., Taghikhani V., Enhanced Heavy Oil Recovery Using TiO_2 Nanoparticles: Investigation of Deposition during Transport in Core Plug, *Energy & Fuels*, **29(1)**: 1–8 (2014).

[21] Kedir A.S., Seland J.G., Skauge A., Skauge T., Nanoparticles for Enhanced Oil Recovery: Influence of pH on Aluminum-Cross-linked Partially Hydrolyzed Polyacrylamide-Investigation by Rheology and NMR, *Energy & Fuels*, **28(4)**: 2343–2351 (2014).

[22] Suleimanov B.A., Ismailov F.S., Veliyev E.F., Nanofluid for Enhanced Oil Recovery, *J. Pet. Sci. Eng.*, 2011, **78(2)**: 431–437 (2011).

[23] Esfandyari Bayat A., Junin R., Samsuri A., Piroozian A., Hokmabadi M., Impact of Metal Oxide Nanoparticles on Enhanced Oil Recovery From Limestone Media at Several Temperatures, *Energy & Fuels*, **28(10)**: 6255–6266 (2014).

[24] Nguyen P., Fadaei H., Sinton D., Pore-Scale Assessment of Nanoparticle-Stabilized CO_2 Foam for Enhanced Oil Recovery, *Energy & Fuels*, **28(10)**: 6221–6227 (2014).

[25] Antony J., "Design of Experiments for Engineers and Scientists", Elsevier, (2014).

[26] Chung T.J., "Computational Fluid Dynamics", Cambridge University Press, New York (2010).

[27] Jafari A., Shahmohammadi A., Mousavi S.M., CFD Investigation of Gravitational Sedimentation Effect on Heat Transfer of a Nano-Ferrofluid," *Iran. J. Chem. Chem. Eng. (IJCCE)*, **34(1)**: 87–96 (2015).

[28] Nazghelichi T., Jafari A., Kianmehr M.H., Aghbashlo M., CFD Simulation and Optimization of Factors Affecting the Performance of a Fluidized Bed Dryer, *Iran. J. Chem. Chem. Eng. (IJCCE)*, **32(4)**: 81–92 (2013).

[29] Jafari A., Hasani M., Hosseini M., Gharibshahi R., Application of CFD Technique to Simulate Enhanced Oil Recovery Processes: Current Status and Future Opportunities, *Pet. Sci.*, **17(2)**: 1-23 (2019).

[30] Jafari A., Feghhi Pour S. E., Gharibshahi R., CFD Simulation of Biosurfactant Flooding into a Micromodel for Enhancing the Oil Recovery, *Int. J. Chem. Eng. Appl.*, **7(6)**: 353-358 (2016).

[31] Mohammadikhah R., Zahedi Abghari S., Ganji H., Ahmadi Marvast M., Improvement of Hydrodynamics Performance of Naphtha Catalytic Reforming Reactors Using CFD, *Iran. J. Chem. Chem. Eng. (IJCCE)*, **33(3)**: 63–76 (2014).

[32] Byrne M., Jimenez M., Rojas E., Castillo E., Computational Fluid Dynamics for Reservoir and Well Fluid Flow Performance Modelling, *"SPE European Formation Damage Conference:*, Noordwijk, The Netherlands (2011).

[33] Farahani R., Lastiwka M.M., Langer D.C., Demirdal B., Matthews C. M., Jensen J., Reilly A., Corporation E., Farahani A., Assessment and Prediction of Erosion in Completion Systems under Hydraulic Fracturing Operations Using Computational Fluid Dynamics, *"SPE Annual Technical Conference and Exhibition"*, Denver, Colorado, USA (2011).

[34] Shiehnejadhesar A., Scharler R., Mehrabian R., Obernberger I., Development and Validation of CFD Models for Gas Phase Reactions In Biomass Grate Furnaces Considering Gas Streak Formation Above the Packed Bed, *Fuel Process. Technol.*, **139**: 142–158 (2015).

[35] Sohrabi M., Henderson G.D., Tehrani D.H., Danesh A., Visualisation of Oil Recovery by Water Alternating Gas (WAG) Injection Using High Pressure Micromodels-Water-Wet System, *"SPE Annual Technical Conference and Exhibition"*, Dallas, Texas, USA (2000).

[36] Emami Meybodi H., Kharrat R., Ghazanfari M.H. , Effect of Heterogeneity of Layered Reservoirs on Polymer Flooding: An Experimental Approach Using 5-Spot Glass Micromodel, *"Europec/EAGE Conference and Exhibition"*, Rome, Italy (2008).

[37] Gharibshahi R., Jafari A., Haghtalab A., Karambeigi M.S., Application of CFD to Evaluate Pore Morphology Effect in the Nanofluid Flooding for Enhanced Oil Recovery, *RSC Adv.*, **37** (2015).

[38] Gharibshahi R., Jafari A., Ahmadi H., CFD Investigation of Enhanced Extra-Heavy Oil Recovery Using Metallic Nanoparticles/Steam Injection in a Micromodel with Random Pore Distribution, *J. Pet. Sci. Eng.*, **174**: 374–383 (2019).

[39] Dezfully M.G., Jafari A., Gharibshahi R., CFD Simulation of Enhanced Oil Recovery Using Nanosilica/ Supercritical CO_2, *Adv. Mater. Res.*, **1104**: 81–86 (2015).

[40] Jafari A., Zamankhan P., Mousavi S.M., Pietarinen K., Modeling and CFD Simulation of Flow Behavior and Dispersivity Through Randomly Packed Bed Reactors, *Chem. Eng. J.*, **144(3)**: 476–482 (2008).

[41] Gharibshahi R., "Simulation and Investigation of Effective Parameters on Enhanced Oil Recovery Process Using Nanoparticles", Tarbiat Modares University, Tehran, Iran (2014).

[42] Farzaneh S.A., Kharrat R., Ghazanfari M.H., Experimental Study of Solvent Flooding to Heavy Oil in Fractured 5-Spot Micromodels: the Role of Fracture Geometrical Characteristics, *"Canadian International Petroleum Conference"*, Calgary, Alberta, Canada, 1–9 (2008).

[43] Zaytsev I.D., Aseyev G.G., "Properties of Aqueous Solutions of Electrolytes", CRC Press, Florida (1992).

[44] Nogi K., Hosokawa M., Naito M., Yokoyama T., "Nanoparticle Technology Handbook", *Elsevier*, Amsterdam (2012).

[45] Langroudi L.O., Pahlavanzadeh H., Mousavi S.M., Statistical Evaluation of a Liquid Desiccant Dehumidification System Using RSM and Theoretical Study Based on the Effectiveness NTU Model, *J. Ind. Eng. Chem.*, **20(5)**: 2975–2983 (2014).

[46] Rastegar S.O.O., Mousavi S.M.M., Rezaei M., Shojaosadati S.a.A., Statistical Evaluation and Optimization of Effective Parameters in Bioleaching of Metals from Molybdenite Concentrate Using Acidianus Brierleyi, *J. Ind. Eng. Chem.*, **20(5)**: 3096–3101 (2013).

[47] Barkhordari V., Jafari A., Ghazanfari M.H., Gharibshahi R., Enhanced Oil Recovery Using Nanoclay, *The 15th Iranian National Congress of Chemical Engineering*, Tehran, Iran (2015).

[48] Mohd T.A.T., Baco J., Bakar N.F.A., Jaafar M.Z., Effects of Particle Shape and Size on Nanofluid Properties for Potential Enhanced Oil Recovery (EOR), "*MATEC Web of Conferences*", *EDP Sciences*, **69**: 3006 (2016).